Modeling and Simulation of Hybrid Energy System Supplying 3Ø Load and its Power Quality Analysis

Sujit Kumar Bhuyan**, Dr. Prakash Kumar Hota*‡, Dr. Bhagabata Panda***

* Department of Electrical Engineering, Veer Surendra Sai University of Technology, Burla, Dist: Sambalpur, Odisha, India

** School of Electrical Sciences, KIIT University, Bhubaneswar, Odisha, India

*** School of Electrical Sciences, KIIT University, Bhubaneswar, Odisha, India

(sujeet.kumar84@gmail.com, p_hota@rediffmail.com, panda_bhagabat@rediffmail.com)

‡ Corresponding Author: P.K.Hota, Veer Surendra Sai University of Technology, Burla, Dist: Sambalpur, Odisha, India, Tel: +91 663 243126,
Fax: +90 663 2430204, p_hota@rediffmail.com

Received: 03.06.2017 Accepted:22.09.2017

Abstract- The proposed Hybrid Energy System (HES) consists of solar photovoltaic (PV) system, the electrolyzer, the storage tank and the solid oxide fuel cell (SOFC). The HES is used to supply the electricity to the 3Ø load as well as 1Ø load which is synchronized to the grid with the help of voltage source converter (VSC). In this technology when PV power is not sufficient to fulfill the load demand, then SOFC power is utilized to fulfill the required demand. A fuel cell controller is proposed in which a PID controller is used to regulate the amount of hydrogen (H_2) flow through the valve and utilized as a fuel of SOFC. In this paper, H_2 is generated from electrolyzer which takes extra PV energy and water as input elements. The complete modeling of the individual components is simulated in Matlab/Simulink environment and also the results obtained are found to be satisfactory. Then power quality factor is verified for HES as well as 3Ø non-linear load to analyze the quality of power.

Keywords- Harmonic distortion, power quality, PV cell, SOFC, electrolyzer, grid

1. Introduction

The renewable energy sources (RESs) are clean energy sources and more reliable in nature. Photo voltaic energy sources, tidal energy sources, wind energy sources and micro-turbines, etc. are the numerous RESs employed in the hybrid energy system [1-2]. In the current research area, the generation of electric energy is proposed for the rural consumers where there is no grid connection. For such areas RESs is the better solution for generation of decentralized power. For such power generation the combination of hydro, wind and PV are the environmental friendly and cost effective according to [3, 27-28, 33-34]. Innovation of the technology is needed to utilize these RESs for the power generation and to obtain the better efficiency. A HES consisting of combination of PV-wind-diesel is used in [4]. But due to increasing cost of diesel and use of the diesel environmental pollution is created that makes the operation of diesel engine prohibited. A HES consisting of a wind-hydro is connected to the grid where the power converters are used to improve the reliability of the power system [5]. The cost and reliability of the HES for the distant and remote places evaluated by the optimization technique are shown in [6]. Now-a-day's many works have been carried out for the analysis of power quality study of the RES consisting of PV, wind and other renewable sources.

A maximum power point tracking (MPPT) is used in PV system to extract maximum power according to procedure adopted in [7]. In recent years, wind energy system (WES) becomes most important energy generating source. However, WES depended on the natural wind speed. Also maximum power point tracker is used to extract maximum power as shown in [8-9]. The grid integration of renewable energy sources along with its challenges, issues and possible solutions has been described by Anees, *et al* [10]. An efficient voltage regulation scheme for three-phase self-excited induction generator feeding single-phase load in remote locations has been identified by Gao, *et al* [11]. Hasaneen, *et al* [12] have discussed the design and simulation of DC/DC boost converter. A comparison of two MPPT techniques for PV system in Matlab/Simulink has been made by Kondawar, *et al* [13]. [14 & 29] give the information about the interconnecting issues of photovoltaic/wind hybrid system with electric utility using artificial intelligence. An improved power conditioning system for grid integration of photovoltaic solar energy conversion systems has been studied by Molina, *et al* [15]. Murthy, *et al* [16] have developed a microhydel grid independent power generation scheme using induction generators for Indian conditions. A wind energy conversion scheme using a self-excited induction generator has been proposed by Raina, *et al* [17]. Fault analysis of grid connected photovoltaic system has been studied by Hota, *et al* [18]. A novel hybrid integrated wind-PV micro co-generation energy scheme for village electricity has been discussed by Sharaf, *et al* [19]. Doron [20] has presented the definition of total harmonic distortion and its effect on measurement interpretation. Then the Power Quality Factor (PQF) describes the power transfer quality of the 3Ø supply connected to the load [21].

In this paper, modeling and simulation is done for a novel HES consisting of PV, electrolyzer, SOFC and storage Tank. Then this HES is connected to the grid by means of VSC in order to achieve continuous power supply to the load. A fuel cell controller is considered for the HES consisting of a PID controller and a valve, where the PID controller is used to control the valve because the flow of hydrogen to the SOFC is regulated through the valve according to the load requirement. The advantages HES connected to the grid make the uninterrupted power supply to the load. From the literature survey it appears that not much research has been done on power quality analysis of HES consisting of PV, electrolyzer and fuel cell. To analyze the power quality a single indicator known as power quality factor (PQF) is considered. It can be mentioned that the quality of low power transfer is caused due to the supply voltage (voltage harmonics or unbalanced voltage supply) or due to the load (unbalanced or nonlinear load) or due to both of them. So, PQF gives quick assessment of the quality of the transfer power at any selected point of the supply. Hence, the power quality analysis is considered to calculate the quality of power transfer of the HES supplying 3Ø non-linear load.

2. Description of Grid Connected Hybrid Energy System

The proposed HES model is given in Fig.1. In this model, it is shown that the PV with maximum power point tracker (MPPT) tracks the maximum output power which is given to the DC/DC converter (boost converter) to increase the DC voltage. Then this voltage is given as the input of DC/AC converter, which converts DC voltage to AC voltage and this AC voltage is used to fulfill the load requirement. The extra power if any is given to the electrolyzer which converts water into H_2 and oxygen. Hence, H_2 is used as a fuel of SOFC and the amount of flow of H2 to SOFC is regulated by the PID controller through the valve. When the PV power is not sufficient to fulfill the load demand then SOFC fulfills the required demand. Also, the HES is connected to the grid through VSC. In this chapter PQF analysis is done to measure the quality of power which is supplied to the 3Ø non-linear load from HES.

2.1 Modeling of Photovoltaic (PV) System

Basically, a PV cell is a p-n junction semiconductor diode where the sun energy falls on the PV cell surface, then it produces the DC power. By using the eq. (1) the PV model is designed. Fig.2 shows the single diode model of PV array and Table 1 contains specifications of the photovoltaic (PV) array. Sun power SRP- 305-WHT solar panel is chosen for modeling and simulation by the help of Matlab according to [18, 25, 26, 30-32].

$$V_{pv} = \frac{N_s akT}{q} \ln\left[\frac{I_{sc} - I_{pv} + N_p}{N_p I_o}\right] - \frac{N_s}{N_p} R_s I_{pv} \qquad (1)$$

Parameters used to design the PV model:

I_0 : Reverse saturation current of PV cell, [A]
I_{SC} : short-circuit PV cell current, [A]
I_{PV}/I_{ph} : Output current of PV cell, [A]
k : Boltzmann's constant, [J/^{o}K]
a : completion or ideality factor
q : electron charge, [C]
R_P : PV cell containing parallel resistance, [Ω]
R_S : PV cell containing series resistance, [Ω]
N_S : No. of series cells in a string of the PV cell
N_P : No. of parallel strings
T : Temperature of the PV cell, [K]
V_{PV} : PV cell terminal voltage in volt, [V]
V_{MP} : The voltage related to maximum power of the PV ccell, [V]
V_{OC} : PV cell open-circuit voltage in volt, [V]

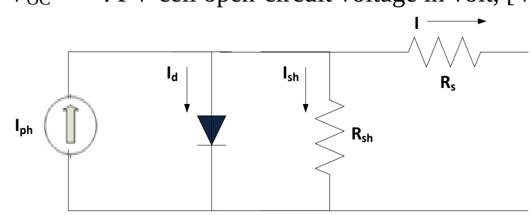

Fig. 2. Single diode model of the PV Array

Table 1 Specifications of photovoltaic (PV) array

Specification	*Value*
No. of series connected PV cell	96
No. of Modules in parallel	66
No. of Modules in series	05
Open circuit voltage(V_{OC})	64.2 V
Short circuit current(I_{SC})	5.96 A
Maximum Power of PV cell	305W
Temperature(T)	25
Irradiance	1000

2.2 Modeling of Electrolyzer

The water is decomposed into hydrogen (H_2) and oxygen through the electrolyzer by using the extra power of PV. The electrolysis equation of water is represented below:

$$H_2O(l) + electrical\ energy = H_2(g) + \frac{1}{2}O_2(g) \qquad (2)$$

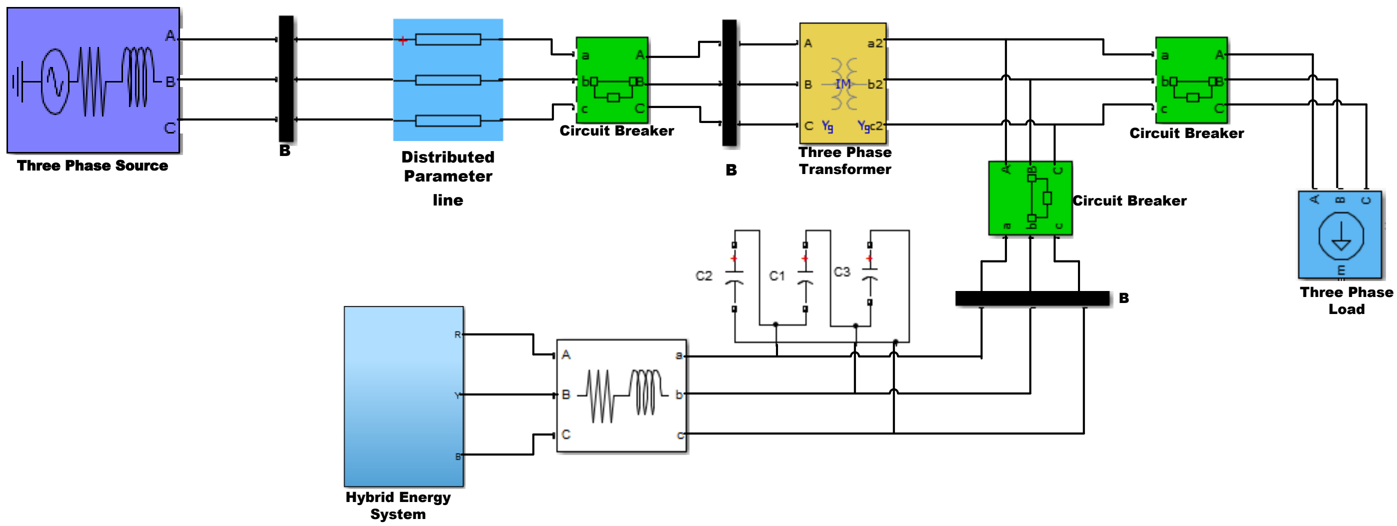

Fig. 1. The proposed model of hybrid energy system connected to grid

Parameters of an electrolyzer model are given below:

i_e : Current of an electrolyzer, [A]
n_c : No. of series connected electrolyzer cells
nH_2 : Amount of hydrogen generated in moles per second, [mol s^{-1}]
F : Faraday constant, [C kmol^{-1}]
η_F : Faraday efficiency

According to Faraday's law, there is direct relation between hydrogen production through the electrolyzer and electrical current given below [25].

$$nH_2 = \frac{n_F n_c i_e}{2F} \quad (3)$$

Faraday efficiency is given in terms of hydrogen generation and its theoretical value which is shown below.

$$\eta_F = 96.5e^{\left(\frac{0.09}{i_e} - \frac{75.5}{i_e^2}\right)} \quad (4)$$

Fig. 3 shows the model of electrolyzer by using the eqs. (3) and (4).

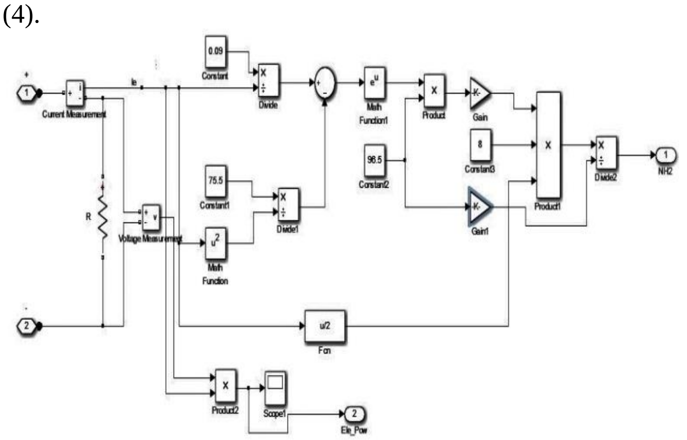

Fig. 3. A brief model of electrolyzer using Simulink

2.3 Modeling of Storage Tank

Storage tank is used to store the H_2, which is generated from the electolyzer. Further this H_2 is used as a fuel of SOFC. Eq. (5) shows the design model of storage tank.

$$P_b - P_{bi} = z\frac{NH_2 RT_b}{MH_2 V_b} \quad (5)$$

Parameters of the storage tank are given below:

Z : Pressure compressibility factor
NH_2 : Amount of hydrogen stored in the storage tank in moles per second, [kmol s^{-1}]
MH_2 : Hydrogen molar mass, [kg kmol^{-1}]
Tb : operating temperature, [^{o}K]
P_{bi} : Storage tank pressure at initial stage, [Pa]
P_b : Storage tank pressure, [Pa]
R : Rydberg/Universal gas constant, [J (kmol ^{o}K) $^{-1}$]
V_b : Storage tank volume, [m^3]

A model of hydrogen storage tank is shown in Fig.4.

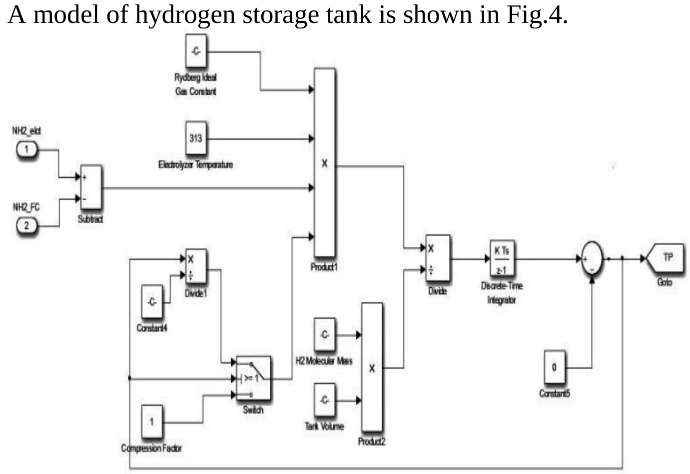

Fig. 4. A brief model of hydrogen storage tank using Simulink

2.4 Modeling of SOFC

SOFC parameters are shown below that has been used to design the model of SOFC [23].

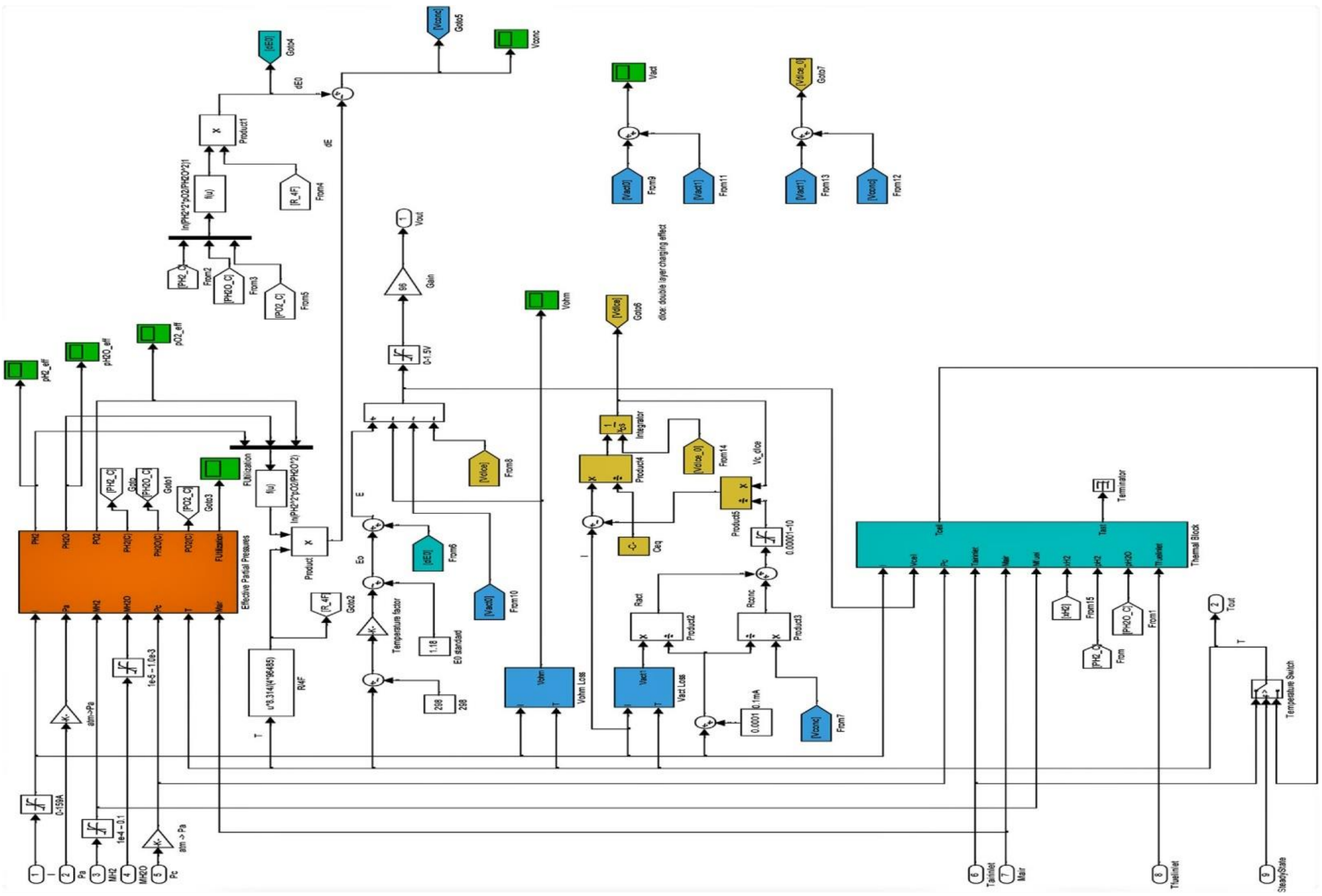

Fig. 5. A brief model of SOFC system using Simulink

B and C : Activation voltage constants are used to simulate SOFC system, [V]
CV : conversion factor, $\left[\frac{\text{Hydrogen(kmol)}}{\text{Methane(Kmol)}}\right]$
E_0 : normal no load voltage, [V]
E : Nernst immediate voltage, [V]
F : Faraday's constant, [C ($kmol^{-1}$)]
I_{FC} : feedback current of SOFC, [A]
k_1 : gain of PI (proportional-integral)
Kan : anode valve constant, $\left[\sqrt{\text{kmol kg}}(\text{atm s})^{-1}\right]$
K_r : modeling constant, [kmol SA^{-1}]
K_{H2O} : molar constant of water valve, [kmol ($atms^{-1}$)]
K_{H2} : molar constant of hydrogen valve, [kmol (atm s^{-1})]
K_{O2} : molar constant of oxygen valve, [kmol (atm s^{-1})]
M_{H2} : hydrogen molar mass, [kg $kmol^{-1}$]
P_{H2O} : water fractional pressure, [atm]
P_{H2} : hydrogen fractional pressure, [atm]
P_{O2} : oxygen fractional pressure, [atm]
N_0 : No. of fuel cells are in series in a stack
q_{H2} : molar flow of hydrogen, [$kmols^{-1}$]
$q_{methane}$: methane flow rate, [$kmols^{-1}$]
q_{O2} : input molar flow of oxygen, [$kmols^{-1}$]
q_{H2}^{in} : input flow of hydrogen, [$kmols^{-1}$]
q_{H2}^{out} : hydrogen output flow, [$kmols^{-1}$]
q_{H2}^{r} : hydrogen flow amount that reacts,[$kmols^{-1}$]
q_{H2}^{req} : hydrogen flow amount that meets load change, [$kmols^{-1}$]
R : Rydberg (Universal) gas constant, [(1atm) (kmol K) $^{-1}$]
R_{int} : internal resistance of SOFC, [Ω]
T : absolute temperature, [K]
U : utilization rate τ
V_{an} : volume of the anode, [m^3]
V_{cell} : SOFC dc output voltage, [V]
τ_1, τ_2 : reformer time constants, [s]
τ_3 : PI controller time constant, [s]
τ_{H2} : hydrogen time constant, [s]
τ_{H2O} : water time constant, [s]
τ_{O2} : oxygen time constant, [s]
Z_{act} : activation over voltage, [V]
Z_{ohmic} : ohmic over voltage, [V]

The ratio of the molar flow of hydrogen and hydrogen partial pressure in a channel is given in [23].

$$\frac{q_{H2}}{P_{H2}} = \frac{K_{an}}{\sqrt{M_{H2}}} = K_{H2} \tag{6}$$

Three factors are considered for the hydrogen flow namely hydrogen input and output flow and hydrogen flow at the time of reaction [22]. So, the required equation is developed as:

$$\frac{d}{dt}p_{H2} = \frac{RT}{V_{an}}\left(q_{H2}^{in} - q_{H2}^{out} - q_{H2}^{r}\right) \quad (7)$$

The flow of reacted hydrogen is shown below [22].

$$q_{H2}^{r} = \frac{N_0 I_{FC}}{2F} = 2K_r I_{FC} \quad (8)$$

The partial pressure of hydrogen is shown below by using Laplace transform of the eqs. (6) and (8).

$$P_{H2} = \frac{1/K_{H2}}{1+\tau_{H2}s}\left(q_{H2}^{in} - 2K_r I_{Fc}\right) \quad (9)$$

where, $\tau_{H2} = \frac{V_{an}}{K_{H2}RT}$ (10)

The output voltage of SOFC can be determined by considering the activation over voltage, Nernst's voltage and the ohmic over voltage as given in [22].

$$V_{cell} = E + \eta_{act} + \eta_{ohmic} \quad (11)$$

Where,

$$\eta_{act} = -Bln(CI_{FC}) \quad (12)$$

And

$$\eta_{ohmic} = -R^{int}I_{FC} \quad (13)$$

So, Nernst voltage is obtained which is given in [22].

$$E = N_O\left[E_O + \frac{RT}{2F}log\left[\frac{P_{H2}\sqrt{P_{O2}}}{P_{H2O}}\right]\right] \quad (14)$$

The SOFC takes H_2 as a fuel for the required power demand. The continuous supply of hydrogen is possible with the help of the reformer. The modeling of the reformer is given in eq. (15).

$$\frac{q_{H2}}{q_{methanol}} = \frac{CV}{\tau_1\tau_2 s^2 + (\tau_1+\tau_2)s + 1} \quad (15)$$

SOFC output current is used as the input of the SOFC to determine the required amount of hydrogen that flow to the SOFC.

$$q_{H2}^{req} = \frac{N_O I_{FC}}{2FU} \quad (16)$$

The available hydrogen of the reformer further utilized to maintain flow of methane by using the PI controller. It can be expressed as:

$$q_{methane} = \left(k_1 + \frac{k_1}{\tau_3 s}\right)\left(\frac{N_O I_{FC}}{2FU} - q_{H2}^{in}\right) \quad (17)$$

Table 2 Specifications of SOFC to design the mathematical mode

Specification	*Value*
Activation voltage constant (B)	0.04777 [A^{-1}]
Activation voltage constant (C)	0.0136 [V]
Conversion factor (CV)	2
Faraday's constant (F)	96 484 600 [$Ckmol^{-1}$]
FC system internal resistance (R_{int})	0.26664 [Ω]
FC absolute temperature (T)	343 [K]
Hydrogen time constant (τ_{H2})	3.37 [s]
Hydrogen valve constant (K_{H2})	4.22 x10^{-5} [kmol (s atm)$^{-1}$]
Hydrogen–oxygen flow ratio(r_{H2O})	1.168
Kr constant =N_0/4F	2.2802 x 10^{-7} [kmol (s A)$^{-1}$
Line reactance (X)	0:0809 [Ω]
Methane reference signal ($Q_{methref}$)	0.000015 [kmol s^{-1}]
No load voltage (E_o)	1.18 [V]
Number of cells (N_o)	88
Number of stacks (N_S)	1
Oxygen time constant (τ_{O2})	6.74 [s]
Oxygen valve constant, (k_{O2})	2.11 x10^{-5} [kmol (s atm)$^{-1}$]
PI gain constant (k_1)	0.25
Reformer time constant (τ_1, τ_2, τ_3)	15 [s]
Universal gas constant (R)	8314.47 [J kmolK^{-1}]
Utilization factor (U)	0.8
Water time constant (τ_{H2O})	18.418 [s]
Water valve constant (K_{H2O})	7.716 x 10^{-6} [kmol (s atm)$^{-1}$]

A SOFC with the range of 5 KW is developed by the help of the above parameters as given in Table 2 and a SOFC model is shown in Fig.5 as given in [24]. For this proposed model three 5 KW SOFC are used.

2.5 Internal Structure of Proposed Hybrid Energy System

Fig.6 shows the internal structure of the proposed hybrid energy system (HES) which is represented in Fig.1. PV system with MPPT tracks the maximum power, which is further utilized to fulfill the required demand of the load. The electrolyzer connected across the buck converter used the extra amount of PV power to extract the H_2 from water according [6]. Hence, this H_2 is used for the fuel of SOFC. A DC-DC converter is connected to PV with MPPT to increase the voltage; also this converter is triggered by the MPPT generated gate pulse. Again another DC/DC converter is used to increase the voltage level of SOFC as shown in Figs.6 and 7. From the Fig.6, it can be seen that the HES is connected to grid with the help of voltage source converter (VSC) to synchronize the HES voltage with the grid voltage. VSC contains two controlled cascade loops that are described below.

Voltage controller of DC-link: Active power and its desired value is controlled by the DC-link voltage controller. i_d* of the DC-link PI controller is used as a reference which is compared with the i_d shown in Fig.8.

Internal current loop: The grid voltage (V_a, V_b, V_c) and grid current (i_a, i_b, i_c) are transformed to *d-q* reference frame with the help of *abc/dq* controller or synchronous reference frame (SRF). DC values are determined by using the SRF because these values are easier to control and design. Hence, these are used for controlling the variables. Phase angle is derived by the PLL (phase locked loop), where grid voltage acts as the input of PLL.

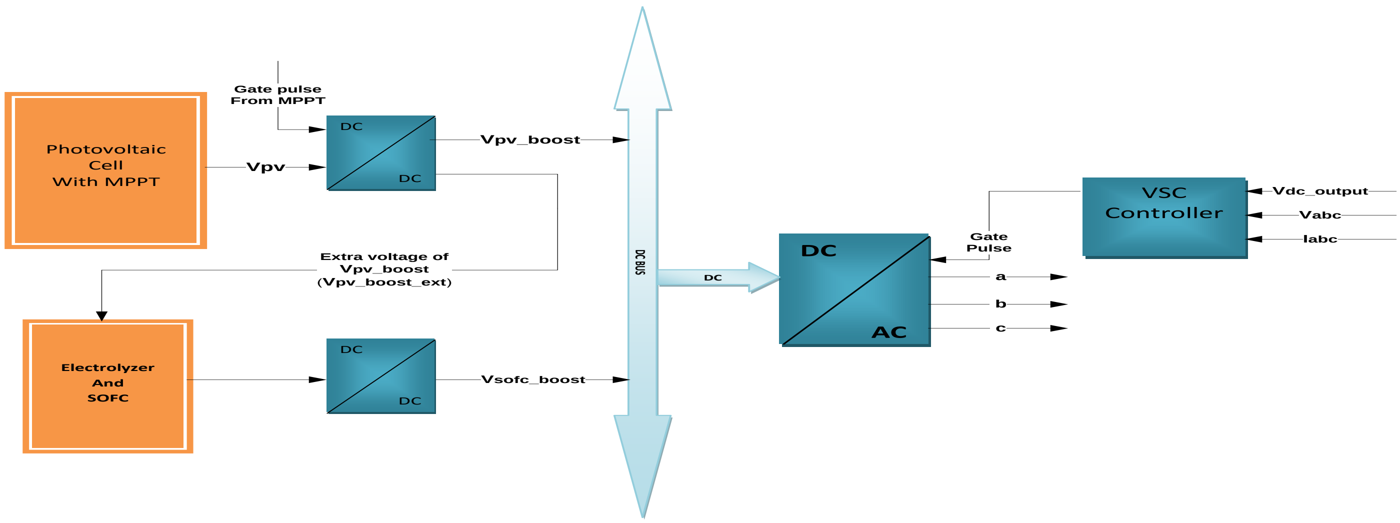

Fig. 6. Block diagram of hybrid energy system (HES)

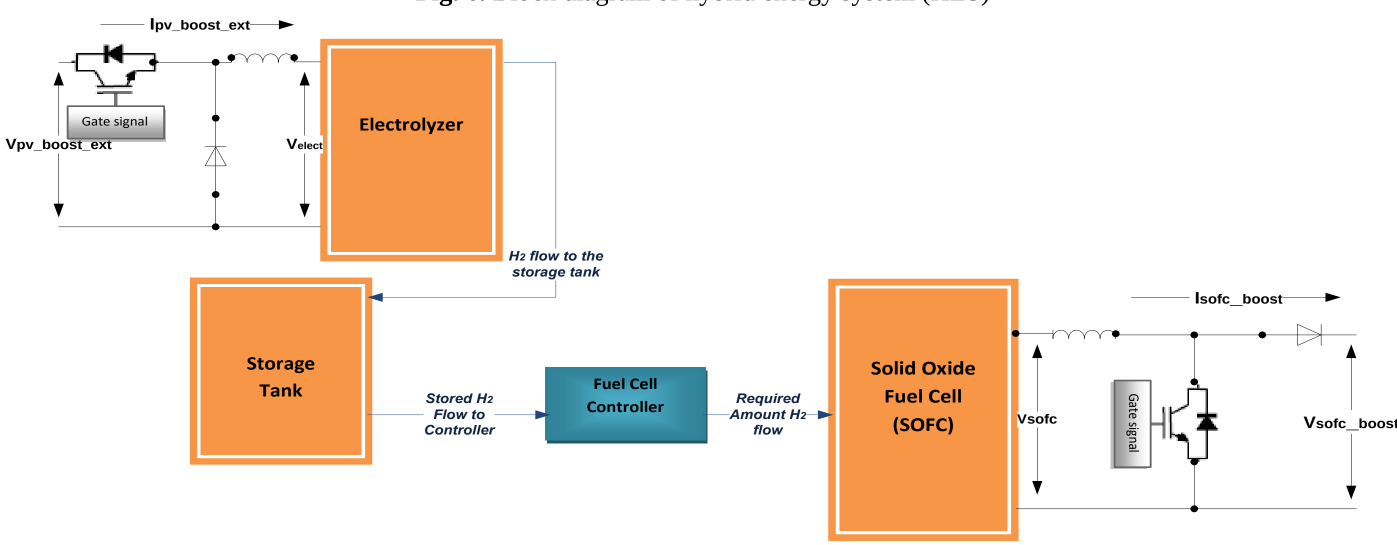

Fig. 7. Block diagram representation of hydrogen flow from electrolyzer to SOFC

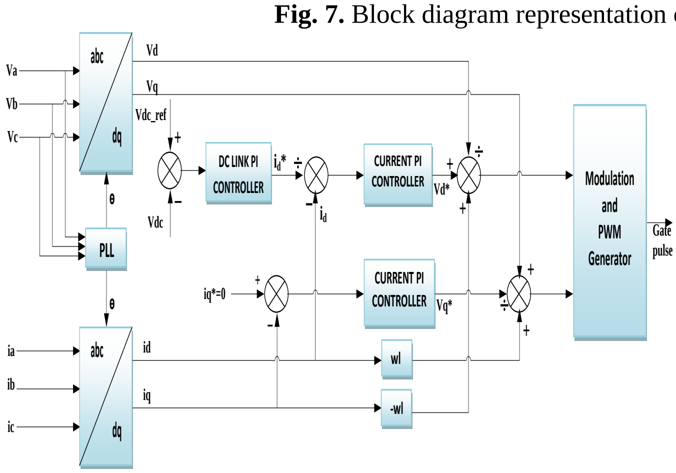

Fig. 8. Block diagram representation of voltage source inverter (VSC)

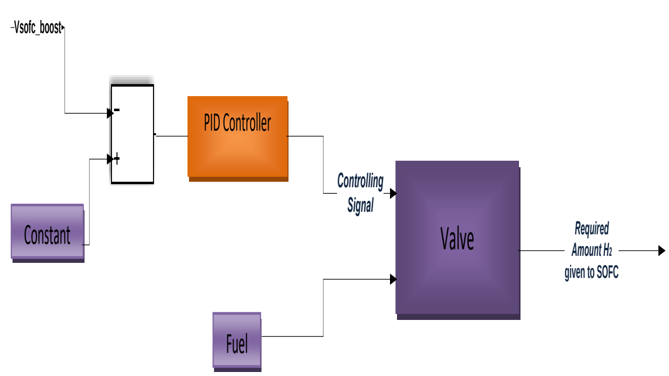

Fig. 9. Block diagram representation of fuel cell controller

As shown in Fig.8, the reference frame voltages (V_d,V_q) are synchronized with the controlled currents. Further i_q*(reference reactive current) is set to zero value as shown in Fig.8. Hence, power factor is to maintain as unity. The voltages (V_d*, V_q*) of the current PI controllers are used as the input of the PWM generator, which produces pulses to trigger the DC/AC converter [24].

Fig.7 shows that an electrolyzer is connected to buck converter, which takes the PV power and that power further utilized by the electrolyzer to convert the water into H_2 and oxygen. Then this H_2 is used as fuel of SOFC to fulfill the load requirement when the PV power is not sufficient for the required load and the rest amount of hydrogen is stored in storage tank for future requirement. Fig.9 represents fuel cell controller block diagram. In this block *Vsofc_boost* (voltage of boost converter connected to SOFC) is compared with the constant value and given to the PID controller. The output signal of the PID controller controls the valve, where the amount of H_2 flows according to the load demand. The PID controller values are set by the help of self tuned mode provided in the PID controller block (P=0.00013317, I = 3.3925227e-05, D = -6.254254172870e-05).

3. Operational Control Strategy of Hybrid Energy System

Operational control strategy is used to manage the correlation between the HES and load demand. It attends the 4 possible ways to supervise the proposed system.

(i) If Load power (Pload) < PV power (Ppv), at that time PV power carry out the load demand and the extra amount of PV power is utilized by the electrolyzer, which converts water into H_2 and oxygen and later this H_2 is used as a fuel of SOFC.

(ii) If Load power (Pload) > PV power (Ppv), at that time PV is not enough to fulfill the required load. So, SOFC is used to fulfill the required demand with PV.

(iii) If Load demand (Pload) = PV power (Ppv), at that time PV power satisfy the required load. So, no extra power is supplied to electrolyzer.

(iv) If PV power (Ppv) is zero, at that time PV does not supply any power. So, required load demand is fulfilled by the SOFC.

In this manner the operational control strategy operates. In case the PV as well as SOFC fails to supply the power, then the grid continuously supplies to the load and provides the uninterrupted power supply to the load.

4. Analysis of Power Quality Factor (PQF)

The power quality factor (PQF), a single indicator ranging from 0 to 1 is used to measure the quality of power transfer of a HES connected to grid supplying the 3Ø load. The aspects considered for power quality are: harmonic levels of the voltage and current; unbalanced 3Ø voltage and current; and phase displacement factor of different phases on the basis of their fundamental frequency. The PQF is unity when a balanced sinusoidal voltage and current is supplied by the network at the zero phase displacement. PQF depends on the following three aspects described below.

A. Harmonics levels of the voltage and current

VTHD and ITHD are the voltage and current total harmonic distortions respectively for a 3Ø or a 1Ø circuits.

$$[VTHD]^2 = \frac{\sum_{h\neq 1} V_h^2}{V_1^2} \quad (18)$$

$$[ITHD]^2 = \frac{\sum_{h\neq 1} I_h^2}{I_1^2} \quad (19)$$

where, V and I represent rms values; h and 1 represents the harmonic order and fundamental, respectively.

Lower order harmonics cause lesser losses than the higher order harmonics with the same amplitude. So, the voltage and current total adjusted harmonics distortion are given below.

$$[VTHD]_{H-A}^2 = \frac{\sum_{k\neq 1} (C_h V_h)^2}{V_1^2} \quad (20)$$

$$[ITHD]_{H-A}^2 = \frac{\sum_{k\neq 1} (D_h I_h)^2}{I_1^2} \quad (21)$$

where, C_h, D_h = weighting factors (> 1).

Eqs.(18) and (19) can be extended to a 3Ø network as given in [21].

$$V_{eH}^2 = \sum_{h\neq 1} \frac{V_{ah}^2 + V_{bh}^2 + V_{ch}^2}{3} \quad (22)$$

$$I_{eH}^2 = \sum_{h\neq 1} \frac{I_{ah}^2 + I_{bh}^2 + I_{ch}^2}{3} \quad (23)$$

V_{eH}, I_{eH} = equivalent harmonics rms voltage and current of the 3Ø network. The eqs. (22) and (23) are used in (20) and (21). Hence, the equivalent adjusted harmonics values are formed that is given below.

$$V_{eH-A}^2 = \sum_{h\neq 1} C_h^2 \frac{V_{ah}^2 + V_{bh}^2 + V_{ch}^2}{3} \quad (24)$$

$$I_{eH-A}^2 = \sum_{h\neq 1} D_h^2 \frac{I_{ah}^2 + I_{bh}^2 + I_{ch}^2}{3} \quad (25)$$

So, QA_1 and QA_2 are the quality aspects of total harmonics destruction of voltage and current (VTHD and ITHD) of the 3Ø network.

$$QA_1 = VTHD = \frac{V_{eH-A}}{V_{e1}} \quad (26)$$

$$QA_2 = ITHD = \frac{I_{eH-A}}{I_{e1}} \quad (27)$$

where, V_{e1}, I_{e1} = equivalent fundamental phase voltage and current of the 3Ø network.

$$V_{e1}^2 = \frac{V_{a1}^2 + V_{b1}^2 + V_{c1}^2}{3} \quad (28)$$

$$I_{e1}^2 = \frac{I_{a1}^2 + I_{b1}^2 + I_{c1}^2}{3} \quad (29)$$

Eqs. (22) to (25), (28) and (29) show about the losses of the 3Ø network. So, some assumptions are shown below:

(1) At a particular frequency the losses of line as well as equipment are related to square of the particular voltage and current.

(2) Parameters of line as well as equipment are symmetrical.

B. Unbalanced 3Ø voltage and current

In a 3Ø networks the power transfer quality is affected due to the unbalanced current and voltage; also many aspects are responsible for this, these are line losses occurs at the same power level, additional losses are occurred in the overloading neutral conductors as well as in drives in a 4-wire distribution system. So, a 3Ø sinusoidal voltage network [V_a,V_b,V_c] is decomposed into following three parts.

$$\left.\begin{aligned}\underline{V^+} &= \frac{1}{\sqrt{3}}\left(\underline{V_a} + a\underline{V_b} + a^2\underline{V_c}\right)\\ \underline{V^-} &= \frac{1}{\sqrt{3}}\left(\underline{V_a} + a^2\underline{V_b} + a\underline{V_c}\right)\\ \underline{V^0} &= \frac{1}{\sqrt{3}}\left(\underline{V_a} + \underline{V_b} + \underline{V_c}\right)\end{aligned}\right\} \tag{30}$$

where, $\underline{V}$ = phasor of V and $a = \exp(j2\pi/3)$. So from eqs. (28) to (30) equivalent voltage is found out.

$$V_{e1}^2 = \underline{V^{+}}^2 + \underline{V^{-}}^2 + \underline{V^{0}}^2 \tag{31}$$

Also the current equations can be written in same manner as voltage is written in eqs (30) and (31). Hence, the quality aspects [QA_3 and QA_4] can be identified as unbalanced voltage and current factors.

$$QA_3 = \frac{[V_{e1}^2 - (\underline{V^+})^2]^{\frac{1}{2}}}{V_{e1}} \tag{32}$$

$$QA_4 = \frac{[I_{e1}^2 - (\underline{I^+})^2]^{\frac{1}{2}}}{I_{e1}} \tag{34}$$

C. *Phase displacement factor of different phases on the basis of their fundamental frequency.*

In the power transfer situation phase displacement among the voltage and current at fundamental frequency gives the information about the utilization of the equipment of the generation as well as distribution. Traditionally in the 1Ø situation the power factor (*pf*) can be expressed as the ratio of the active power (*P*) and the apparent power (*S*), also the power is the rms voltage and current.

But, in non-sinusoidal case power factor above described to be confusing. So, according to [21] instantaneous power is the product of voltage and current instantaneous values. Hence, the active power (*P*) is derived from the averaging of instantaneous power with respected to time. But, there is no physical meaning of the apparent power (*S*), hence the voltage and current values are not considered at each instant. When instantaneous voltage and current uphold a constant ratio; at that time apparent power (*S*) equals to *P*.

All the incompleteness and ambiguities written above can be avoided when a physical entity is directly responsible for utilization of the poor power capacity at the considered fundamental frequency. Hence, the phase difference occurs in the voltage and current having the fundamental frequencies at the load side or source side. So, this aspect is reflected in the power quality and hence, a new factor is considered known as orthogonal current factor (*OCF*) according to [21].

$$OCF = \frac{I_{1a}sin_{\emptyset 1a} + I_{1b}sin_{\emptyset 1b} + I_{1c}sin_{\emptyset 1c}}{I_{1a} + I_{1b} + I_{1c}} \tag{34}$$

$$QA_5 = |OCF| \tag{35}$$

where, I_{1a}, I_{1b} and I_{1c} = rms values of phase currents at the fundamental frequency. $\emptyset_{1a}$, $\emptyset_{1b}$ and $\emptyset_{1c}$ = phase differences between voltages and currents at fundamental frequency components.

PQF (a single measurable indicator) is used to reflect different various power quality aspects according to [21] that can be expressed as:

$$PQF = \sum_i w_i(1 - QA_i) \tag{36}$$

where, w_i = weighting factor ($\cong$ 1).It is different for the different consumers and recommendation of the weighting factor is supported by the economics studies according to [21]. It can be chosen to show economical and technical priorities in different environments.

QA_i = different quality aspects

The PQF is unit or ideal when the loaded network is balanced having sinusoidal voltages and currents with phase displacement is zero. PQF value is low due to the poor uses of the power capacity of the source or due to the harmonics containing higher level or due to unbalance between different phases.

5. Simulation Results and Discussion

The proposed HES described above has been designed in MATLAB/Simulink environment and also the performance characteristics of this system are verified on different conditions. Hydrogen (H_2) generation from the electrolyzer is

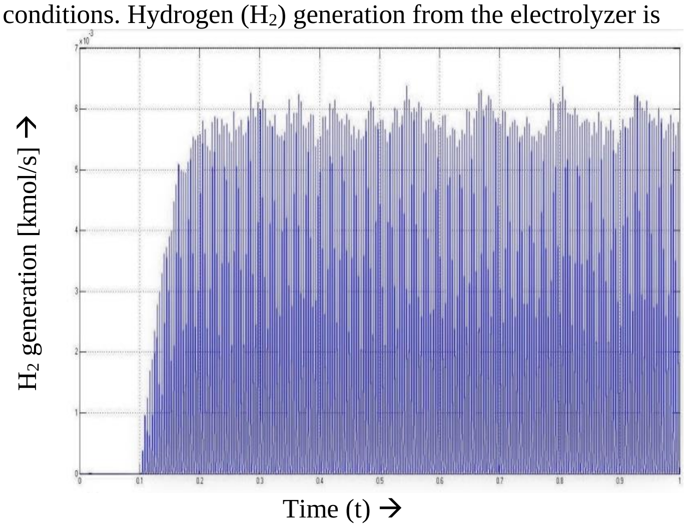

Fig. 10. H_2 generation by Electrolyzer

achieved by taking the extra amount of PV power shown in Fig.10 and this hydrogen is used as fuel of the fuel cell (SOFC) because this hydrogen is used to flow to SOFC through the valve which is shown in Fig.11a to fulfill the required demand when the PV power is not sufficient to fulfill the requirement load. Hence, the hydrogen flow through the valve is controlled by the PID controller. Accordingly, Fig.11b shows the output of the PID controller.

Output voltage of a 5KW SOFC is shown in Fig.12a. Three nos. of 5KW SOFC are connected in series, whose output voltage is shown in Fig.12b.

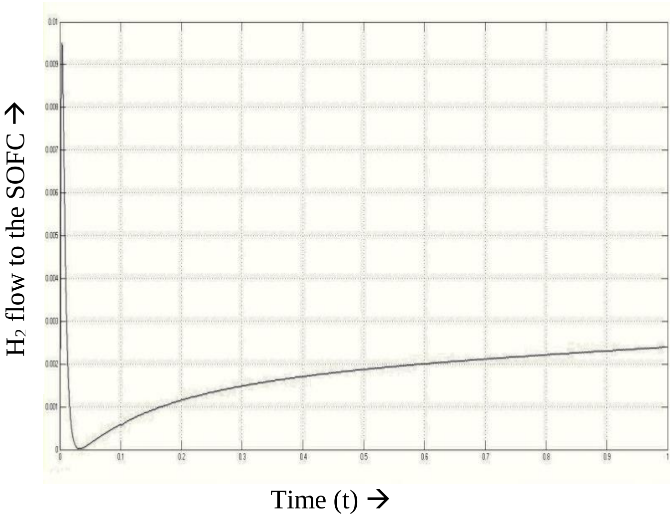

Fig. 11a. H_2 flow to the SOFC

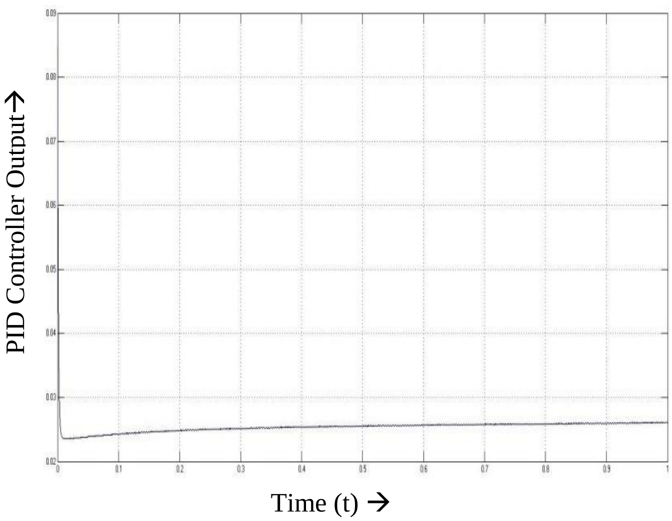

Fig. 11b. PID Controller Output

Fig. 11. A detailed observation of H_2 flow to SOFC and its control

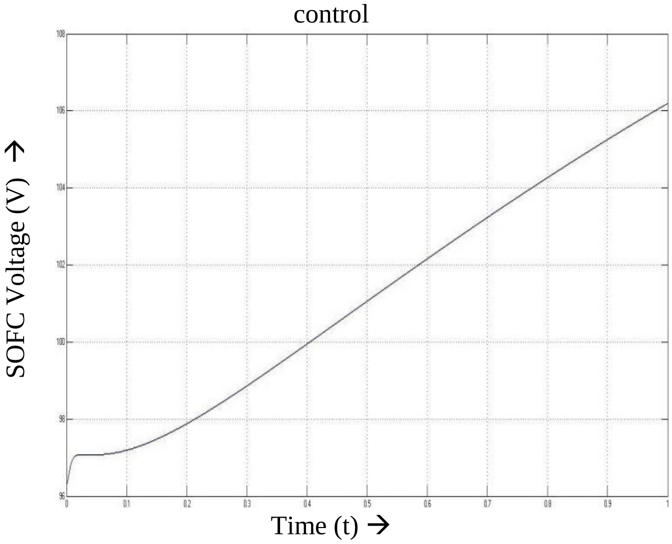

Fig.12a. Output voltage of a 5 KW SOFC

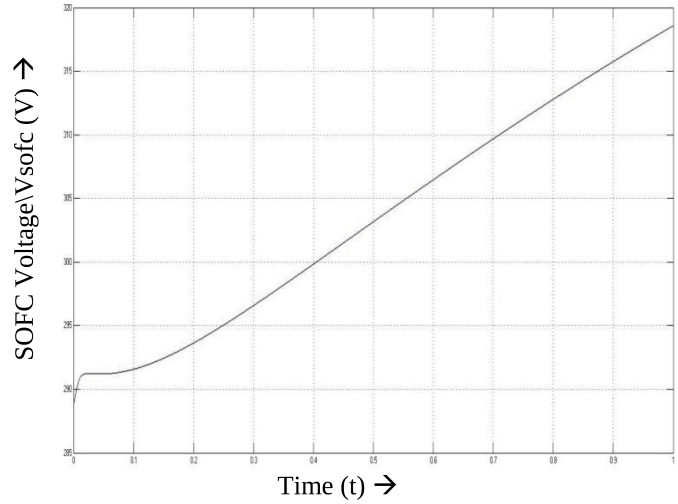

Fig.12b. Output voltage of 3 nos. of 5KW SOFC

Fig.12. Output voltage of the SOFC

Output voltage of a 5KW SOFC is shown in Fig.12a. Three nos. of 5KW SOFC are connected in series, whose output voltage is shown in Fig.12b.

This output voltage of SOFC is increased by the help of boost converter (DC/DC converter) as shown in Fig.13 and used for fulfilling the demanded load; when PV power is not sufficient. Fig.14 shows the waveforms for the voltage and current of HES supplied to the 3Ø non-linear load. Similarly, Fig.15 shows the waveforms for voltage, current and power of a 3Ø non-linear load with the active power (P) = 8000W, inductive power (Q_L) = 2000VAR and capacitive power (Q_C) = 100VAR. Hence, this HES is used to fulfill the 3Ø load demand. Also, HES is used for domestic purposes and gives the clean energy sources. Further, HES is cheaper when it is used for a domestic purpose in a colony based system, when more than 3 consumers are supplied by the HES system connected to grid.

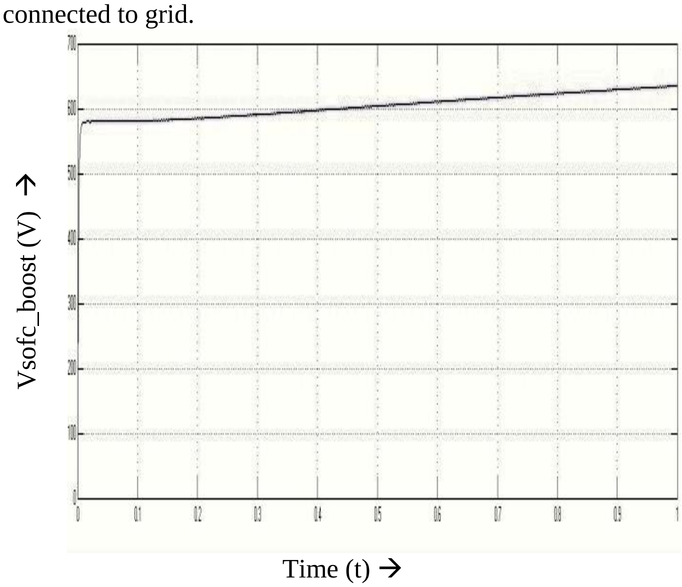

Fig. 13. Output voltage of boost converter connected to SOFC

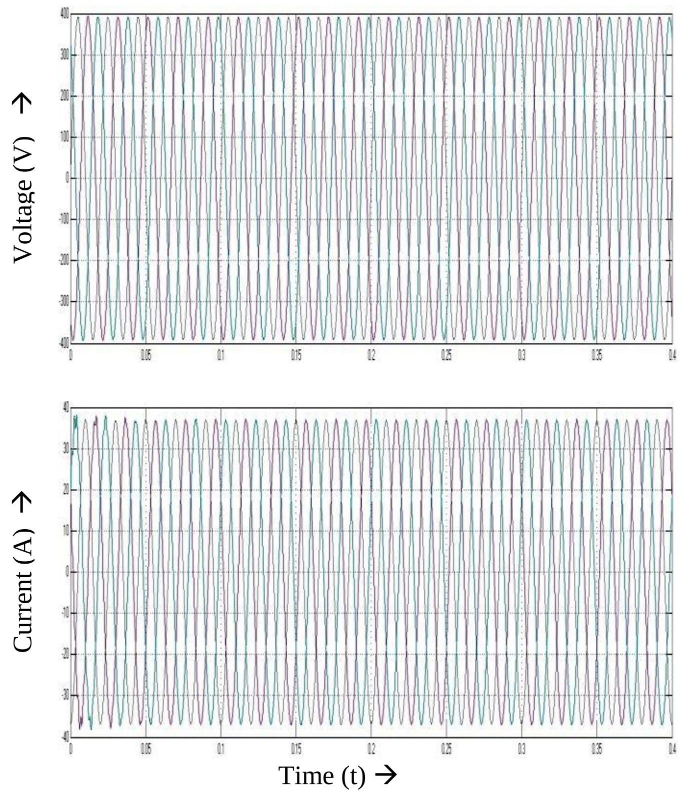

Fig. 14. Output voltage and current of hybrid energy system (HES)

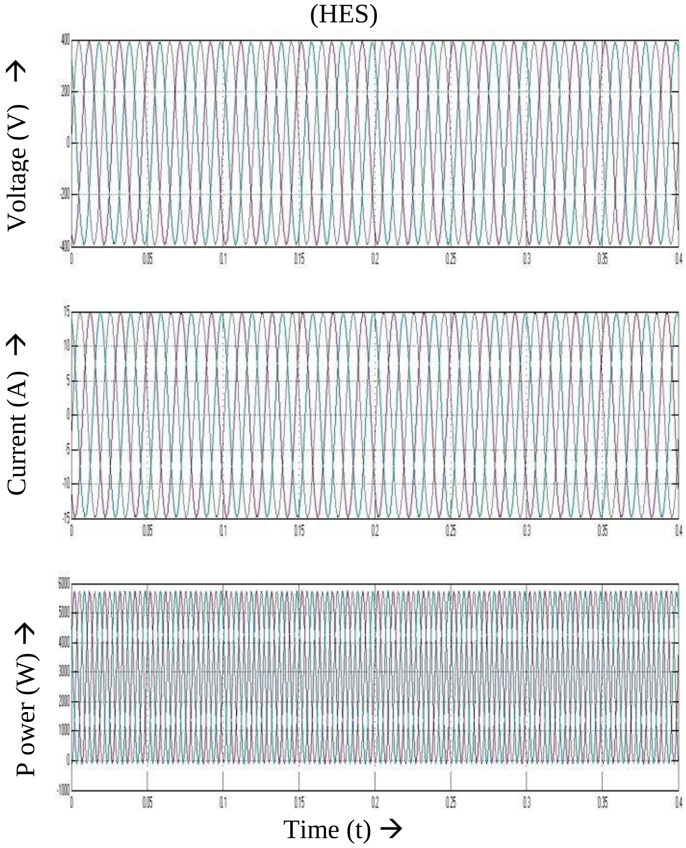

Fig. 15. Voltage, current and power of a 3Ø non-linear load

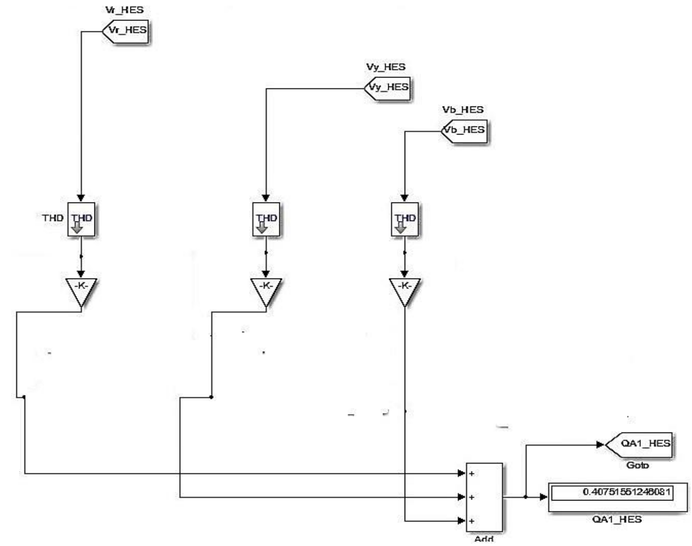

Fig. 16. QA_1 of the HES

The power quality analysis is verified in this paper for the HES and 3Ø load to find out the quality of power. The QA_1, QA_2, QA_3, QA_4 and QA_5 of the HES as described in eqs. 26, 27, 32, 34 and 35 respectively, are simulated by the help of Matlab/Simulink. Fig.16 represents the model of QA_1, where the value of QA_1 is found to be 0.4075155. In this manner QA_2 value of 0.3100727, QA_3 value of 0.7072647, QA_4 value of 0.7072647 and QA_5 of 2.74128507 of the HES are obtained. Hence, Fig.17 shows the PQF, whose value is found to be 95.1265972. Also, the PQF analysis of the 3Ø load is done and verified to be same as those of HES.

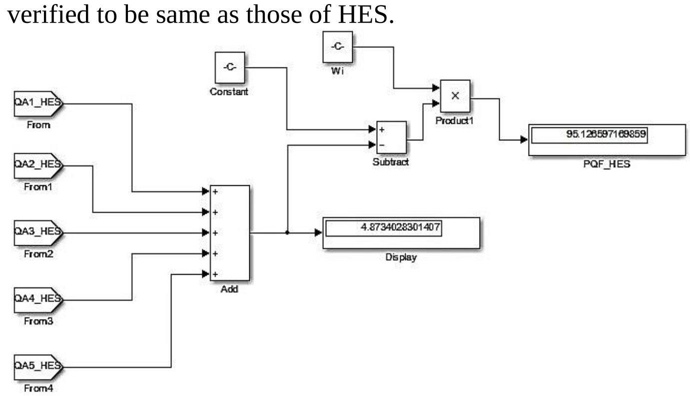

Fig. 17. PQF of the HES

The values of power quality analysis of the 3Ø non-linear load are found to be as QA_1 = 0.4074447, QA_2 = 0.4644307, QA_3 = 0.7072625, QA_4 = 0.7540068, QA_5 = 2.74128507 and PQF = 94.92557. Fig.18 shows the PQF the 3Ø non-linear load.

6. Conclusion

This paper presents a HES consisting of PV/FC/Electrolyzer with a storage tank. Different type of characteristics as well as system configuration of the various

HES sections are verified under simulation. Overall controls as well as power management strategy are also highlighted in this paper. The proposed system is clean and environmental friendly system, where PV is used to generate the power, which is utilized for the 3Ø as well as 1Ø load and the extra energy source of PV if any is utilized for the production of H_2, which in the later stage is used as a fuel of SOFC. This SOFC is used when PV power is not sufficient for the load demand. Also this paper gives the information about the flow of H_2 to the SOFC through the valve that is controlled by the PID controller. Finally, PQF analysis is done for the HES and 3Ø non-linear load as the necessity of this PQF analysis is to measure the quality of power transfer.

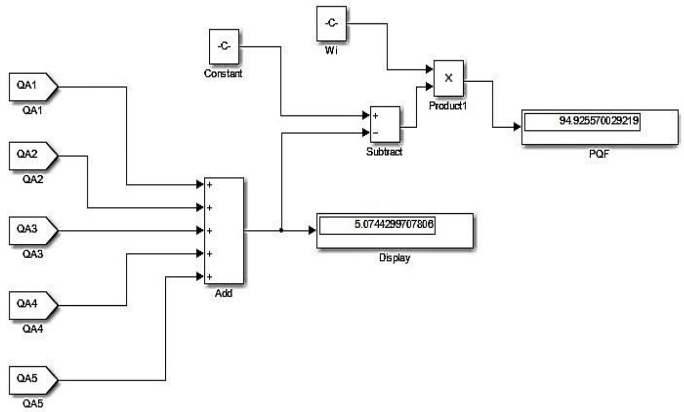

Fig. 18. PQF of the 3Ø non-linear load

References

[1] S. Tamalouzt, N. Benyahia, T. Rekioua, R. Abdessemed, "Performances analysis of WT-DFIG with PV and fuel cell hybrid power sources system associated with hydrogen storage hybrid energy system", International Journal of Hydrogen Energy, Vol. 41, pp. 21006-21021, 2016.

[2] R. W. Mosobi, T. Chichi, S. Gao, "Power quality analysis of hybrid renewable energy System", Cogent Engineering, Vol. 2, pp. 1-15, 2015.

[3] M. F. Nejad, M. A. M.Radzi, M. Z. A. A.Kadir, H. Hizam, "Hybrid renewable energy systems in remote areas of equatorial countries", Proceedings of the 2012 IEEE Student Conference on Research & Development (SCOReD), Pulau Pinang, pp. 11-16, December 2012.

[4] M. S. H. Lipu, M. S. Uddin, M. A. R. Miah, "A feasibility study of solar-wind-diesel hybrid system in rural and remote areas of Bangladesh", International Journal on Renewable Energy Resource, Vol. 3, pp. 895-900, 2013.

[5] P. K. Goel, B. Singh, S. S. Murthy, N. Kishore, "Isolated wind-hydro hybrid system using cage generator and battery storage", IEEE Transactions on Industrial Electronics, Vol. 58, pp. 1141-1153, 2011.

[6] M. Bansal, D. K. Khatod, R. P. Saini, "Modeling and optimization of integrated renewable energy system for a rural site", Proceedings of the 2014 International Conference on Reliability, Optimization and Information Technology (ICROIT), pp. 25-28, February 2014.

[7] R. K. Gera, H. M. Rai, Y. Parvej, H. Soni, "Renewable energy scenario in India: Opportunities and challenges", Indian Journal of Electrical and Biomedical Engineering, Vol. 1, pp. 10-16, 2013.

[8] M. G. Villalva, J. R. Gazoli, E. Ruppert, "Modelling and circuit based simulation of photovoltaic arrays", Proceedings of 2009 Power Electronics Conference, Brazil, pp. 1244-1245, 2009.

[9] M.G.Villalva, J.R.Gazoli, E.Filho, "Comprehensive approach to modeling and simulation of photovoltaic arrays", IEEE Transactions on Power Electronics, Vol. 24, pp. 1198-1208, 2009.

[10] A. S. Anees, "Grid integration of renewable energy sources: Challenges, issues and possible solutions", Proceedings of 2012 International Conference on Power Electronics (IICPE), Delhi, pp. 1-6, 2012.

[11] S.Gao, G.Bhuvaneswari, S.S.Murthy, U.K.Kalla, "Efficient voltage regulation scheme for three-phase self excited induction generator feeding single-phase load in remote locations", IET Renewable Power Generation, Vol. 8, pp. 100-108, 2014.

[12] B. M. Hasaneen, A. A. E. Mohammed, "Design and simulation of DC/DC boost converter", Proceedings of 2012 IEEE Power System Conference, Aswan, pp. 335-340, 2012.

[13] S. S. Kondawar, U. B. Vaidya, "A Comparison of two MPPT techniques for PV system in Matlab/Simulink", International Journal of Engineering Research and Development, Vol.2, pp.73-79, 2012.

[14] A. A. E. Mohammed, "Study of interconnecting issues of photovoltaic/wind hybrid system with electric utility using artificial intelligence", Ph.D Thesis, Faculty of Electrical Engineering Department, Minia University, Minya, 2006.

[15] M. G. Molina, E. C. D. Santos, M. Pacas, "Improved power conditioning system for grid integration of photovoltaic solar energy conversion systems", Proceedings of 2010 International Transmission and Distribution Conference and Exposition, Latin America, pp. 163-170, 2010.

[16] S. S. Murthy, R. Jose, B. Singh, "Experience in the development of microhydel grid independent power generation scheme using induction generators for Indian conditions", Proceedings of 1998 IEEE Conference on Global Connectivity in Energy, Computer, Communication and Control, Vol. 2, pp. 461-465, 1998.

[17] G. Raina, O. P. Malik, "Wind energy conversion using a self-excited induction generator", IEEE Transactions on Power Apparatus and System, Vol. 102, pp. 3933-3936, 1983.

[18] P. K. Hota, B. Panda, B. Panda, "Fault analysis of grid connected photovoltaic system", American Journal of Electrical Power and Energy Systems, Vol.5, pp.35-44, 2016.

[19] A. M. Sharaf, M. A. H. El-Sayed, "A novel hybrid integrated wind-PV micro co-generation energy scheme for village electricity", Proceedings of the 2009 International Electric Machine and Drives Conference (IEMDC), pp. 1244-1249, 2009.

[20] S. Doron, "On the definition of total harmonic distortion and its effect on measurement interpretation", IEEE Transaction on Power Delivery, Vol. 20, pp. 526-528, 2005.

[21] D. Sharon, J. Montaño, A. López, M. Castilla, D. Borrás, J. Gutiérrez , "Power Quality Factor for networks supplying unbalanced nonlinear loads", IEEE Transactions on Instrumentation and Measurement, Vol. 57, pp. 1268-1274, 2008.

[22] M. G. Molina, E. J. Espejo, "Modeling and simulation of grid-connected photovoltaic energy conversion systems", International Journal of Hydrogen Energy, Vol. 39, pp. 8702-8707, 2014.

[23] M. Uzunoglu, O. C. Onar, "Static VAR compensator based reactive power Management for SOFC power plants", International Journal of Hydrogen Energy, Vol. 33, pp. 2367-2378, 2008.

[24] G. K. Bayrak, M. Cebeci, "Grid connected fuel cell and PV hybrid Power generating system design with Matlab Simulink", International Journal of Hydrogen Energy, Vol. 39, pp. 8803-8812, 2014.

[25] M. Uzunoglu, O. C. Onar, M. S. Alam, "Modeling, control and simulation of a PV/FC/UC based hybrid power generation system for stand-alone applications", Renewable Energy, Vol. 34, pp. 509–520, 2009.

[26] B. K. Bijaykant, S. Minz, "Intelligent Control Algorithm for Maximum Power Point Tracking of PV Arrays", International Journal of Innovative Research in Science, Engineering and Technology, Vol. 5, pp. 18913-18922, 2016.

[27] H. S. Das, A. Dey, T. C. Wei, A. H. M. Yatim, "Feasibility Analysis of Standalone PV/Wind/Battery Hybrid Energy System for Rural Bangladesh", International Journal of Renewable Energy Research, Vol.6, pp. 402-412, 2016.

[28] V. O. Okinda, N. A. Odero, "Modelling, Simulation and Optimal Sizing of a Hybrid Wind, Solar PV Power System in Northern Kenya", International Journal of Renewable Energy Research, Vol.6, pp. 1199-1211, 2016.

[29] K. D. Mercado, J. Jimenez, G. Christian, M. Quintero, "Hybrid Renewable Energy System based on Intelligent Optimization Techniques", International Conference on Renewable Energy Research and Applications , pp. 661-666, Birmingham, UK, 2016.

[30] B. Shalavadi, V. Ravindranadh, R. Y. Udaykumar, "Modelling and Analysis of a Standalone PV/Micro Turbine/ Ultra Capacitor Hybrid System", International Journal of Renewable Energy Research, Vol.6, pp. 847-855, 2016.

[31] L. Rao, S. Paragond, C. P. Kurian, B. K. Singh, "Design and Simulation of Solar and Wind Energy Conversion System in Isolated Mode of Operation", International Conference on Renewable Energy Research and Applications , pp. 999-1004,Palermo,Italy,2015.

[32] M. D. T. Ahemad, T. Goncalves, M. Tlemcani, "Single Diode Model Parameters Analysis of Photovoltaic Cell", International Conference on Renewable Energy Research and Applications, pp. 396-400, Birmingham, UK, 2016.

[33] J. Zhang, D. Guo, F. Wang, Y. Zuo, H. Zhang, "Research on Energy Management Strategy for Islanded Microgrid Based on Hybrid Storage Device", International Conference on Renewable Energy Research and Applications, pp. 91-96, Madrid, Spain, 2013.

[34] A. Z. AKTAS, "A Review and Comparison of Renewable Energy Strategies or Policies of Some Countries" International Conference on Renewable Energy Research and Applications, pp. 636-643, Palermo, Italy, 2015.